



MISCONCEPTION OF TOTAL HARMONIC DISTORTION IN RESOLVERS

R. Alipour-Sarabi, Z. Nasiri-Gheidari*, and H. Oraee

Department of Electrical Engineering, Sharif University of Technology, Tehran, Iran

**Corresponding author, Email: znasiri@sharif.edu*

Abstract

Resolvers, as magnetic position sensors, are increasingly used in motion-control systems. Due to electro-magnetic structure, they preserve more accurate and reliable operation than optical encoders in stressful conditions. Usually, to evaluate the performance of a resolver, total harmonic distortion (THD) of output signals is calculated. In this study, by using analytical expressions, it is shown that THD of output signal is not a reliable indicator of the performance of a resolver.

Keywords: Electromagnetic Sensors, Estimated Position Error, Resolver, Total Harmonic Distortion (THD).

1. INTRODUCTION

Position sensors are widely used in almost all motion-control systems. In industry, the two well-known position sensors are encoders and resolvers [1], [2]. Contrary to encoders, resolvers provide absolute position over one revolution/translation [3] and thanks to resolvers' analog output signals. They suggest infinite resolution [4]. Moreover, resolvers, due to their ability to work in harsh and polluted environments, low sensitivity to temperature and pressure variations, and simple structure, have found wide applications in aviation, robotics and automation, motor drives, and electric vehicles [5]-[7]. Fig. 1 shows the structure of a typical 2-pole rotary resolver. Generally, resolvers are comprised of two sets of coils; excitation and signal coils. By feeding the excitation coil, located on the moving part, with a high frequency sinusoidal voltage, a voltage is induced in the output coils, called signal windings [8]. Signal windings are physically 90 degrees apart. Therefore, the induced voltages are proportional to the sine and cosine of the relative position of the moving and stationary parts. Additionally, there is a rotary transformer to transfer the excitation voltage V_r to the moving part. Output signals, V_s and V_c , are then fed to an electronic Resolver to Digital Converter (RDC) [9]-[10]. In fact, the function of RDC is to find the envelope of output

signals and calculate the position of moving part (θ). Accordingly, studies in the field of resolvers are categorized into two branches. While the first groups of studies are devoted to the magnetic structure of resolver, the other ones focus on the RDC.

Symbol	Quantity
B_M	maximum of magnetic flux density
B_P	maximum of fundamental(P^{th}) magnetic flux density
B_{P-ki}	maximum of $(P - ki)^{th}$ harmonic of magnetic flux density
f_e / ω_e	excitation voltage frequency / angular speed
α	an arbitrary position in the air-gap
S	a surface located between the moving and stationary parts
∂S	is the boundary of surface S
E	electric field
v	velocity of the boundary ∂S
$V_r / V_s / V_c$	Excitation / Sin / Cos winding voltage
V_e / V_m	RMS value of Excitation / Sin and Cos winding
ω_m	angular(mechanical) speed of moving part
θ	instantaneous position of moving part
M_{rs}	mutual inductance of moving and stationary parts
I_m	RMS value of excitation winding current
P	pole pairs of resolver as an electrical machine

The studies intend to minimize the estimated position error by modifications in the magnetic design of resolver and/or suppressing error in the electronic part by using compensators. Resolvers, due to manufacturing imperfections, slotting effects, tooth harmonics, coils' overhang leakage flux, mechanical misalignments, and winding topology, experience some voltage harmonics in the output signals [11]. Despite the fact that RDC is able to compensate some errors, machine designers are eager to reduce these errors at their origin. The most common approach for performance evaluation of a resolver is to measure the analog signals' THD [12]. Investigations have frequently used the THD and harmonic contents of output signals as a reliable index to evaluate the performance of a resolver [2]-[8], [11]-[16]. If *performance* is defined as the accuracy of estimated position, then it will be shown that the THD of analog signals is not a reliable indicator of a resolver *performance*.

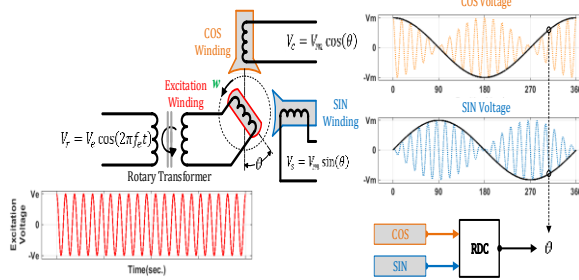


Fig.1. BASIC STRUCTURE OF A TYPICAL 2-POLE ROTARY RESOLVER

2. BASIC FORMULATION

When the rotor is excited with high frequency sinusoidal voltage, magnetic flux density in the air-gap is:

$$B(t) = B_M \cos(2\pi f_e t - \alpha) \quad (1)$$

The induced voltage in a single loop of a coil is obtained by Faraday's law, as:

$$\begin{aligned} e(t) &= \int_{\partial S} (E + v \times B) \cdot dl \\ &= \int_S \frac{\partial B}{\partial t} dS + \oint_{\partial S} v \times B \cdot dl \end{aligned} \quad (2)$$

The signal windings are connected to a high impedance RDC, which leads to small currents in output windings. Thus, the output currents can be neglected in calculations. Using (2), the output signals of resolver are obtained as:

$$\begin{aligned} V_s(t, \theta) &= V_m \sin(\theta) \cos(\omega_e t) \\ &+ \frac{\omega_m}{\omega_e} V_m \cos(\theta) \sin(\omega_e t) \end{aligned} \quad (3)$$

$$\begin{aligned} V_c(t, \theta) &= V_m \cos(\theta) \cos(\omega_e t) \\ &- \frac{\omega_m}{\omega_e} V_m \sin(\theta) \sin(\omega_e t) \end{aligned} \quad (4)$$

$$V_m = \omega_e M_{rs} I_m \quad (5)$$

The first terms on the right-hand side of (3) and (4) correspond to the transformer EMF and the second to the motional EMF. Given that the excitation frequency is 5 to 50 times of the angular speed, the motional EMF can be neglected. On the other hand, due to the slotting effect and non-ideal winding distribution, the air-gap's magnetic flux density and, consequently, the mutual inductance between excitation and signal windings is rich in harmonics. In a resolver with $2P$ poles, $h = P$ corresponds to the order of fundamental component of output voltage. In this essence, (3), (4) and (5) can be rewritten as:

$$\begin{aligned} V_s &= V_s(t, \theta) = \sum_{h=1}^{\infty} V_h \sin\left(\frac{h}{P}\theta\right. \\ &\quad \left.+ \varphi_h\right) \cos(\omega_e t) \end{aligned} \quad (6)$$

$$\begin{aligned} V_c &= V_s(t, \theta + \frac{\pi}{2}) = \sum_{h=1}^{\infty} V_h \sin\left(\frac{h}{P}\theta + \varphi_h\right. \\ &\quad \left.+ \frac{h\pi}{2P}\right) \cos(\omega_e t) \end{aligned} \quad (7)$$

$$V_h = \omega_e M_{rs,h} I_m \quad (8)$$

Where h is a representation for harmonic order. Since the phase of harmonics are calculated with reference to the fundamental one, without losing the generality, φ_P is assumed to be zero. In this study harmonics refers to all its types including sub-harmonics and inter-harmonics.

3. PROBLEM DEFINITION

As discussed in the earlier section, one way to evaluate the estimated position accuracy is to measure the output signals' THD, as:

$$\begin{aligned} THD &= \frac{\sqrt{V_{rms}^2 - V_P^2}}{V_P} \\ &= \frac{\sqrt{\sum_{h=1}^{\infty} V_h^2 - V_P^2}}{V_P} \end{aligned} \quad (9)$$

The estimated position is calculated using (10):

$$\theta_{est.} = \tan^{-1}\left(\frac{V_s}{V_c}\right) \quad (10)$$

Fig. (2) shows the output voltage waveform and the estimated position profile when 11th harmonic exist in the output voltages. As seen from Fig. (2), presence

of unwanted harmonics leads to a deviation in the estimated position profile. Nevertheless, presence of harmonics is not the only factor that affects the performance of a resolver.

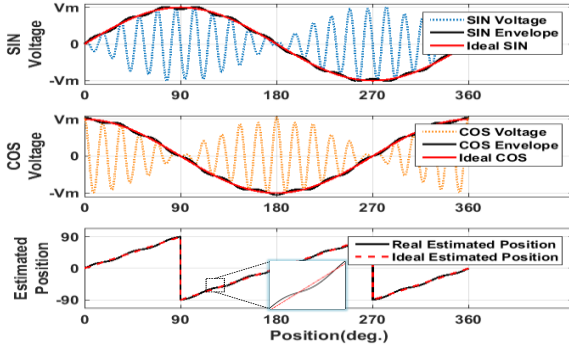


Fig. 2. WAVEFORMS OF SINE AND COSINE SIGNALS AND ESTIMATED POSITION IN PRESENCE OF HARMONICS IN OUTPUT SIGNALS.

Logical connection among voltage harmonics plays a major role in determining the estimated position error which is not included in THD. In this regard, (6) and (7) can be rewritten as:

$$V_s = \cos(\omega_e t) \left\{ V_p \sin(\theta + \varphi_p) + \sum_{h=1}^{P-1} \left[\frac{V_h + V_{2P-h}}{2} \left(\sin\left(\frac{h}{P}\theta + \varphi_h\right) + \sin\left(\frac{2P-h}{P}\theta + \varphi_{2P-h}\right) \right) + \frac{V_h - V_{2P-h}}{2} \left(\sin\left(\frac{h}{P}\theta + \varphi_h\right) - \sin\left(\frac{2P-h}{P}\theta + \varphi_{2P-h}\right) \right) \right] + \sum_{h=2P} V_h \sin\left(\frac{h}{P}\theta + \varphi_h\right) \right\} \quad (11)$$

$$V_c = \cos(\omega_e t) \left\{ V_p \sin\left(\theta + \varphi_p + \frac{\pi}{2}\right) + \sum_{h=1}^{P-1} \left[\frac{V_h + V_{2P-h}}{2} \left(\sin\left(\frac{h}{P}\theta + \varphi_h + \frac{h\pi}{2P}\right) + \sin\left(\frac{2P-h}{P}\theta + \varphi_{2P-h} + \frac{(2P-h)\pi}{2P}\right) \right) + \frac{V_h - V_{2P-h}}{2} \left(\sin\left(\frac{h}{P}\theta + \varphi_h + \frac{h\pi}{2P}\right) - \sin\left(\frac{2P-h}{P}\theta + \varphi_{2P-h} + \frac{(2P-h)\pi}{2P}\right) \right) \right] + \sum_{h=2P} V_h \sin\left(\frac{h}{P}\theta + \varphi_h + \frac{h\pi}{2P}\right) \right\} \quad (12)$$

By rearranging:

$$V_s = \cos(\omega_e t) \left\{ V_p \sin(\theta + \varphi_p) + \sum_{h=1}^{P-1} \left[(V_h + V_{2P-h}) \sin\left(\theta + \frac{\varphi_h + \varphi_{2P-h}}{2}\right) \cos\left(\frac{P-h}{P}\theta - \frac{\varphi_h - \varphi_{2P-h}}{2}\right) - \right. \right. \quad (13)$$

$$\left. (V_h - V_{2P-h}) \cos\left(\theta + \frac{\varphi_h + \varphi_{2P-h}}{2}\right) \sin\left(\frac{P-h}{P}\theta - \frac{\varphi_h - \varphi_{2P-h}}{2}\right) \right] + \sum_{h=2P} V_h \sin\left(\frac{h}{P}\theta + \varphi_h\right) \right\}$$

$$V_c = \cos(\omega_e t) \left\{ V_p \cos(\theta) + \sum_{h=1}^{P-1} \left[(V_h + V_{2P-h}) \cos\left(\theta + \frac{\varphi_h + \varphi_{2P-h}}{2}\right) \cos\left(\frac{P-h}{P}\theta - \frac{\varphi_h - \varphi_{2P-h}}{2} + \frac{(P-h)\pi}{2P}\right) + (V_h - V_{2P-h}) \sin\left(\theta + \frac{\varphi_h + \varphi_{2P-h}}{2}\right) \sin\left(\frac{P-h}{P}\theta - \frac{\varphi_h - \varphi_{2P-h}}{2} + \frac{(P-h)\pi}{2P}\right) \right] + \sum_{h=2P} V_h \sin\left(\frac{h}{P}\theta + \varphi_h + \frac{h\pi}{2P}\right) \right\} \quad (14)$$

To study the suitability of THD as an indicator of estimated position error, two assumptions are taken into account:

- *First:* It is well-known that the high order harmonics are smaller in magnitude in comparison with low order ones. To make the calculations straightforward, harmonics with $f \geq 2f_p$ are neglected. This assumption does not affect the generality of the problem. Therefore, (9) is reduced to (15):

$$THD = \sqrt{\frac{\sum_{h=1}^{2P-1} V_h^2 - V_p^2}{V_p^2}} \quad (15)$$

- *Second:* Remaining harmonics have a symmetry around the fundamental one. In other words, $(h)^{th}$ and $(2P-h)^{th}$ components have the following characteristics:

$$V_h = V_{2P-h} \quad (16)$$

$$\left(\varphi_h + \varphi_{2P-h}\right) / 2 = \varphi_p \quad (17)$$

$$\text{hencefore: } THD = \sqrt{\frac{2 \sum_{h=1}^{P-1} V_h^2}{V_p^2}} \quad (18)$$

In the cases where $V_h \neq 0$, (18) is non-zero. The more harmonics are in the output voltages, the higher estimated position error will be. Nevertheless, using (10), (13), (14), and the above mentioned assumptions, the estimated position is calculated as:

$$\begin{aligned} \text{Estimated position error} &= \theta_{est.} - \theta \\ &= \tan^{-1} \left(\frac{1 + \sum_{h=1}^{P-1} \left[\left(\frac{2V_h}{V_P} \right) \cos \left(\frac{P-h}{P} \theta - \varphi_h \right) \right]}{1 + \sum_{h=1}^{P-1} \left[\left(\frac{2V_h}{V_P} \right) \cos \left(\frac{P-h}{P} \theta - \varphi_h + \frac{(P-h)\pi}{2P} \right) \right]} \right) \times \\ &\frac{\sin(\theta)}{\cos(\theta)} - \theta \end{aligned} \quad (19)$$

Eq. (19) shows that if the *second* assumption is met, the estimated position error will be too low. In fact, the first term in parenthesis is close to unity which leads to minor errors. In other words, for a signal whose harmonics have a symmetry around the fundamental harmonic, the presence of those harmonics has less effect on the estimated position error. While, for the other signal whose harmonics have no symmetry around the fundamental, even with the same value of THD, higher estimated position error is expected. This is contrary to the customary use of THD as an index of resolver accuracy.

This conclusion can be explained by rotating magnetic field in the air-gap, too. Fig. (3)-a shows the rotating magnetic field of the fundamental harmonic as well as $(P \pm k_1)^{th}$ and $(P \pm k_2)^{th}$ ones for a typical $2P$ -pole resolver in the rotating $d - q$ frame, where k_1 and k_2 are arbitrary positive integers. If the angular speed of fundamental component ($h = P$) is taken to be w , then the mentioned harmonics will rotate at a speed of $\frac{(P \pm k_1)}{P} w$ and $\frac{(P \pm k_2)}{P} w$, respectively. Accordingly, if the fundamental harmonic is taken as the reference field, then harmonics with $h > P$ and harmonics with $h < P$ rotate in the positive and negative directions with respect to the reference field, respectively. Fig. (3)-b shows phasor diagram of magnetic field in the air-gap when the fundamental harmonic of magnetic field is assumed to be the reference vector. As seen from Fig. (3)-b, in the stationary $\alpha - \beta$ frame, each harmonic has in-phase (B_α) and quadrature (B_β) components. If the *second* assumption is taken into account, the quadrature component of symmetrical

harmonics ($h = P \pm k_i$), will cancel each other. Fig. (3)-c, the resultant magnetic flux density in the stationary $\alpha - \beta$ frame. Symmetry of harmonics lead to the conclusion that the resultant magnetic field density has only in-phase component. Therefore, the induced voltages in the stator that are resulted from total magnetic flux density, contains symmetrical components and, consequently, more accurate estimated position is obtained. Fig. 4 shows normalized output voltages, their harmonic contents and estimated position error for three different cases resulted from a typical 10-pole resolver. Circular curves of output voltages are presented in Fig. 4-a. Presence of various harmonics in the output voltages, beside the fundamental one, lead to deviation from the ideal curve. Ideal curve is obtained if only the 5th harmonic exist. The harmonic content of output voltages is shown in Fig. 4-b. As seen from Fig. 4-b, in Case I the *second* assumption is met such that the symmetrical harmonics with respect the fundamental one contain equal magnitude and equal phases but with a different signs. However, in Case II and Case III the second assumption is violated. All these cases presents 14.76% as the THD of output voltages. However, the estimated position error in Case I is minimum among those shown in Fig. 4-c. The average estimated position error and maximum estimated position error in Case I are 0.028 and 0.093, in Case II 0.104 and 3.130, and in Case III 0.100 and 3.140, all in degrees, respectively.

Beside the above mentioned deficiency of THD as an ideal indicator of estimated position error, it has some further limitations. As seen from (9), THD is not sensitive to the order and the phase of harmonics; however, (10) shows that both those parameters affect the estimated position error. Moreover, quadrature error that is prevalent in resolvers, is not included in THD. In fact, the quadrature error exists when the two output signals are not perpendicular:

$$V_s(t, \theta) = \sum V_{m,(h)} \sin(\theta_h) \cos(\omega_e t) \quad (20)$$

$$V_c(t, \theta) = \sum V_{m,(h)} \cos(\theta_h + \beta) \cos(\omega_e t) \quad (21)$$

where β is the amount of imperfection. While the quadrature error results in an increase in the estimated position error, the THD of output signal does not reflect the presence of this imperfection.

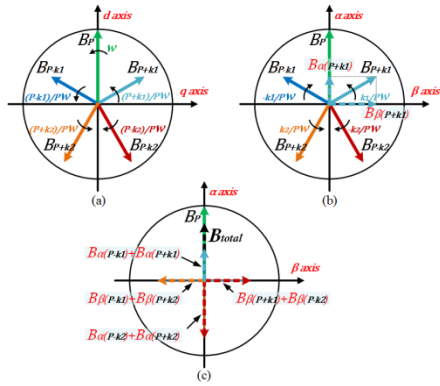


Fig. 3. (a): PHASOR DIAGRAM OF MAGNETIC FLUX DENSITY IN THE AIR-GAP, IN THE ROTATING D-Q FRAME, (b): PHASOR DIAGRAM OF MAGNETIC FLUX DENSITY IN THE AIR-GAP, IN THE STATIONARY α - β FRAME, (c): RESULTANT MAGNETIC FLUX DENSITY.

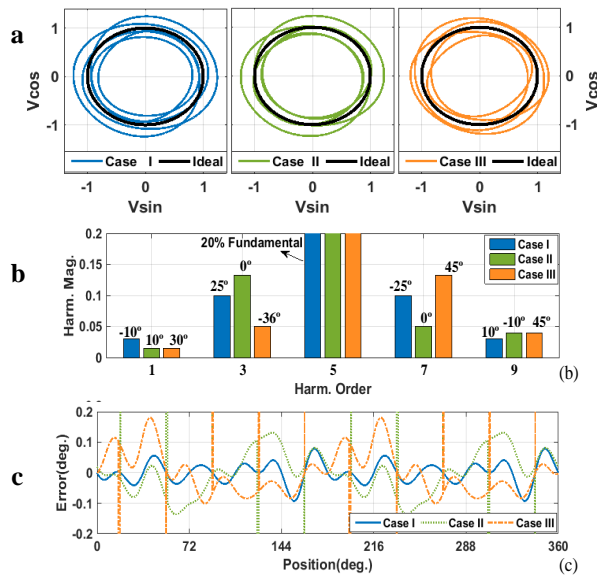


Fig. 4. WAVEFORMS OF SIN AND COS SIGNALS, THEIR HARMONIC CONTENTS AND ESTIMATED POSITION FOR CASE I, II AND III. (a): CIRCULAR CURVE, (b): HARMONIC CONTENTS OF OUTPUT SIGNAL, SAME THDs, DIFFERENT MAGNITUDE AND PHASE, AND (c): ESTIMATED POSITION ERROR

4. CONCLUSION

In this study, the weaknesses of total harmonic distortion, as an index of measuring the accuracy of a resolver, were introduced. Analytical expressions were provided to justify the claim. To sum up: The THD of resolver’s output signals is a good indicator for the quality of estimated position, but it is not a reliable index. This is due to the fact that

THD is not sensitive to the order of harmonics. Therefore, harmonics with different orders but with the same magnitude have identical effects on the THD. However, the estimated position error is a function of harmonics order. Besides, THD is not affected by the phase of harmonics and quadrature error. It is shown that when the disturbing harmonics are symmetrical over the fundamental one, the estimated position error is independent of harmonics magnitude and THD. Therefore, to improve resolver’s performance, a winding arrangement and machine structure should be proposed in such a way that the output signal’s THD become minimum and its harmonic contents have a symmetrical distribution over the fundamental one.

5. REFERENCES

- [1] George Ellis,. 2012. “Control System Design Guide: Using Your Computer to Understand and Diagnose Feedback Controllers, Butterworth-Heinemann”, p: 287, ISBN 978-0-12-385920-4.
- [2] X. Ge, Z. Q. Zhu, R. Ren and J. T. Chen,. 2015."A Novel Variable Reluctance Resolver with Nonoverlapping Tooth–Coil Windings," *IEEE Trans. Energy Convers.*, vol. 30(2), P: 784-794.
- [3] L. Sun,. 2008 "Analysis and Improvement on the Structure of Variable Reluctance Resolvers," *IEEE Trans. Magn.*, vol. 44(8), P: 2002-2008.
- [4] A. Verma, B. Rodriguez,. 2016. “Electrical design considerations for industrial resolver sensing applications”, Available: <http://www.ti.com/lit/wp/slyy100/slyy100.pdf>
- [5] X. Ge, Z. Q. Zhu, R. Ren and J. T. Chen,.2016. "A Novel Variable Reluctance Resolver for HEV/EV Applications," *IEEE Trans. Ind. Appl.*, vol. 52(4), P: 2872-2880.
- [6] X. Ge, Z. Q. Zhu, R. Ren and J. T. Chen, 2015."Analysis of Windings in Variable

- Reluctance Resolver," *IEEE Trans. Magn.*, vol. 51(5), P: 1-10.
- [7] Z. Nasiri-Gheidari, 2017. "Design, Performance Analysis, and Prototyping of Linear Resolvers," *IEEE Trans. Energy Convers.*, vol. 32(4), P: 1376-1385.
- [8] R. Alipour-Sarabi, Z. Nasiri-Gheidari, F. Tootoonchian and H. Oraee, 2017. "Effects of Physical Parameters on the Accuracy of Axial Flux Resolvers," *IEEE Trans. Magn.*, vol. 53(4), P: 1-11.
- [9] D. A. Khaburi, 2012. "Software-Based Resolver-to-Digital Converter for DSP-Based Drives Using an Improved Angle-Tracking Observer," *IEEE Trans. Instrum. Meas.*, vol. 61(4), P: 922-929.
- [10] M. Benammar, A. Khattab, S. Saleh, F. Bensaali and F. Touati, 2017. "A Sinusoidal Encoder-to-Digital Converter Based on an Improved Tangent Method," *IEEE Sensors J.*, vol. 17(16), P: 5169-5179.
- [11] O. A. Tolstykh, A. P. Balkovoi, M. G. Tiapkin and A. S. Markov, 2016. "Research and development of the 4X-variable reluctance resolver," *2016 IEEE NW Russia Young Researchers in Electrical and Electronic Engineering Conference (EIconRusNW)*, St. Petersburg, P: 704-709.
- [12] R. Alipour-Sarabi, Z. Nasiri-Gheidari, F. Tootoonchian and H. Oraee, 2017. "Performance Analysis of Concentrated Wound-Rotor Resolver for Its Applications in High Pole Number Permanent Magnet Motors," *IEEE Sensors J.*, vol. 17(23), P: 7877-7885.
- [13] A. Daniar, Z. Nasiri-Gheidari and F. Tootoonchian, 2017. "Position error calculation of linear resolver under mechanical fault conditions," *in IET Science, Measurement & Technology*, vol. 11(7), P: 948-954.
- [14] Chengjun Liu, Ming QI, and Meng Zhao, 2013. "Analysis of Novel Variable Reluctance Resolver with Asymmetric Teeth on the Stator," *Mathematical Problems in Engineering*, vol. 2013, Article ID 958747, 9 pages.
- [15] Z. Nasiri-Gheidari, R. Alipour-Sarabi, F. Tootoonchian and F. Zare, 2017. "Performance Evaluation of Disk Type Variable Reluctance Resolvers," *IEEE Sensors J.*, vol. 17(13), P: 4037-4045.
- [16] H. Saneie, Z. Nasiri-Gheidari and F. Tootoonchian, 2017. "Analytical model for performance prediction of linear resolver," *in IET Electric Power Applications*, vol. 11(8), P: 1457-1465.